Baseline assessment of the South African sardine resource using data from 1984-2019

C.L. de Moor*

Correspondence email: *carryn.demoor@uct.ac.za*

A quantitative assessment of the South African sardine resource has been updated to include data from 1984 to 2019. This two mixing-component hypothesis assumes no stock recruitment relationship during conditioning. The west component abundance remains at a very low level. The biomass is estimated to be about 20% of the historical (1984-2019) average in November 2019, with a biomass of about 90 thousand tons. The west component spawner biomass is estimated to be below 7 thousand tons (13% of the historical average) and the effective spawner biomass is estimated to be 21 and a half thousand tons (31% of the historical average). The south component abundance is estimated to be higher, at 70% (biomass) to 88% (spawner biomass and effective spawner biomass) of the historical average, with a biomass in November 2019 of about 385 thousand tons.

Introduction

This document presents results for a baseline assessment of South African sardine, using data from 1984-2019. The assessment assumes the sardine population consists of two mixing 'components', with a west component distributed west of Cape Agulhas and a south component distributed south-east of Cape Agulhas. There is movement of fish from the west component into the south component and a small contribution of south component spawning to west component recruitment. The former is modelled by an annually-varying proportion of west component sardine moving to form part of the south component while the latter is modelled by assuming a time-invariant 8% of south component spawner biomass contributes to west component effective spawner biomass.

Population Dynamics Model

The population dynamics model for the South African sardine resource is the same as that of de Moor (2020a), except where allowance has been made to fit to additional data. The data used in this assessment are listed in de Moor *et al*. (2020).

Stock recruitment relationships have been fit to the time series of model estimated spawner biomass and November recruitment using lognormal likelihoods. The stock recruitment relationships for the west component have been estimated excluding the November 2000 to 2002 years of peak recruitment (de Moor *et al.* 2019). Recruitment during those years is assumed to vary about a (higher) median value.

The historical time series of sardine biomass assuming the parameter values fixed at those estimated by the baseline model, but with no historical (1984-2019) catch, i.e. "Dynamic B_0" (de Moor and Butterworth 2009) has also been estimated. To incorporate feedback between spawner biomass and recruitment into this model (the primary driver of the difference between the Dynamic B_0 time series and that of the baseline model), this estimation assumed the Hockey Stick stock recruitment relationship and associated annual residuals estimated after conditioning. As all model parameters, including initial numbers-at-age, are fixed at the values estimated by the baseline model (with catch) when calculating the Dynamic B_0 timeseries, the initial years of the time series are less reliable due to transient effects. This particularly so as the population was not at a stable equilibrium at the start of this time series.

* MARAM (Marine Resource Assessment and Management Group), Department of Mathematics and Applied Mathematics, University of Cape Town, Rondebosch, 7701, South Africa.

Results and Discussion

The model is able to fit the survey estimates of abundance well in most years (Figures 1 and 2). The years for which the model predicted value exceeded the 95% confidence interval of the survey estimate typically corresponded to years for which there is conflicting information between the November biomass and May/June recruit surveys. The relatively high model predicted recruitment on the south coast in May/June 2018 and 2019 are now primarily informed by length frequency data given the absence of survey estimates of recruitment in these recent years.

High proportions of west component fish are still estimated to move to the south component in some recent years, however the primary movement in terms of biomass occurred during the pulse years at the turn of the century (Figure 3).

The model fit to the survey length frequencies (Figures 5, 6, Appendix A) and commercial length frequencies (Figures 8 and 9) is relatively good, with little noticeable change to that achieved by de Moor (2020a), and with similar survey and commercial selectivities to that estimated by de Moor (2020a) (Figures 4 and 7).

Figure 10 shows the growth curves which are modelled to vary by cohort. The average $t_{0,j,y}$ for the von Bertalanffy growth curves for the south component is 0.2 (close to November) with a maximum difference in $t_{0,j,y}$ between cohorts of approximately 9 months. Even with an adjustment to the growth curve for the west component, the average $t_{0,j,y}$ is approximately 7 months before November, with a maximum difference in $t_{0,j,y}$ between cohorts of about 7 months. These ranges are slightly greater than that achieved by de Moor (2020a), and averages further from November, but due to time constraints no alternative adjustments to the growth curve have been tested with these updated data. Figure 11 shows the length-at-age distributions for one example year.

The model estimates relatively low sardine infection by the “tetracotyle” type digenean endoparasite in the most recent years (Figure 12). The model fit to the parasite prevalence data has been updated from that of de Moor (2020a) in some years (e.g. 2011 and 2018) given the inclusion of prevalence data from 7.5 to 9.5cm in addition to the updated and extended time series of other data.

The model estimated November recruitment is plotted against spawner biomass and effective spawner biomass in Figure 14, indicating the low west component [effective] spawner biomass and recruitment in recent years. The west component effective spawner biomass includes 8% of the south component spawner biomass. The proportion of this effective west component spawner biomass that consists of south component spawner biomass is estimated to be high in recent years, reaching 68% in 2019 (Figure 15). This reflects the very low current west component spawner biomass (<7000t in 2018 and 2019).

Although the Beverton Holt stock recruitment relationship provides the best fit to the west component data, and the Hockey Stick stock recruitment relationship provides the best fit to the south component data, there is little preference in terms of model selection criteria between the Hockey Stick, Beverton Holt and Ricker stock recruitment relationships (Table 1, Figure 14).

The updated and extended time series of data has resulted in a downward correction to the de Moor (2020a) estimate of November biomass in 2018 (Table 2, Figures 1 and 16) and a lower estimate of west component recruitment in May/June 2018

(November 2017) (Table 2, Figures 2 and 16). There has also been a downward correction to the 2018 May/June recruitment and November biomass from that estimated by the initial 2019 assessment (de Moor 2019a) that was based on older methodology and used to inform management advice in 2019 (Table 2, Figure 16). This model estimates the effective west and south component spawner biomasses to be 21 500t and 169 500t in November 2019, respectively. de Moor (2019a) had estimated the west and south component spawner biomasses in November 2018 to be 21 000t and 127 800t, respectively (Table 2, Figure 16). Therefore, when considering the west component effective spawner biomass - the biomass of primary concern for future recruitment to the resource as a whole - the population is estimated to be at the same level at that estimated a year ago when catch advice was given for 2019 (de Moor 2019a,b). The (small) increase in west component abundance estimated from 2018 to 2019 corresponds with the lower abundance now estimated for November 2018 compared to that estimated by de Moor (2019a, 2020a).

Figure 17 shows the historical harvest proportion on the sardine, which has often been substantially higher on the west component than on the south component.

Figure 18 shows the Dynamic B_0 and equivalent effective spawner biomass time series against that estimated by the baseline model. These provide an indication of the historical impact of catch on the population. The depletion (baseline biomass and effective spawner biomass relative to that under no historical catch) is also shown. While a similar historical range of depletion is estimated for the west and south components in terms of total biomass, the depletion of the west component effective spawner biomass has been greater than that of the south component effective spawner biomass. West component depletion reached a minimum of 40% in 2007 and is currently estimated at 57% in 2019. A sensitivity test to this Dynamic B_0 time series was estimated assuming the Beverton Holt stock-recruitment relationship. This resulted in a similar depletion range to that estimated assuming the Hockey Stick stock recruitment relationship.

While a Kobe plot cannot currently be given as the SWG-PEL has not (yet) defined target reference points for sardine, Figure 19 plots the historical harvest proportion against relative biomass. The relative biomass considered is both biomass against Dynamic B_0 and effective spawner biomass against carrying capacity as estimated by the Hockey Stick stock recruitment relationship and effective spawner biomass estimated by the Dynamic B_0 model. In developing a target reference point for sardine, it may be prudent to base such on a proportion of the average historical Dynamic B_0. However, movement from the west to the south component and the contribution of south component spawning to west component recruitment complicates the interpretation of these figures in isolation.

In Summary

This document has presented an updated baseline assessment of South African sardine. Only results at the joint posterior mode have been provided thus far, and readers are reminded that there is estimation error about these values. Posterior distributions have not yet been estimated given time constraints. The assessment estimates the west component biomass in November 2019 to be about 90 000t - 20% of the historical (1984-2019) average. The west component spawner biomass is estimated to be below 7 000t (13% of the historical average) and the effective spawner biomass is estimated to be 21 500t (31% of the historical average). The assessment estimates the south component biomass in November 2019 to be about 385 000t which is ~70% of the historical average and the south component spawner biomass and effective spawner biomass are estimated to be at 88% of the historical average at 184 000t and 169 500t, respectively.

References

de Moor CL. 2019a. Revision to the Initial Assessment of the South African sardine resource using data from 1984-2018. DAFF: Branch Fisheries Document FISHERIES/2019/MAR/SWG-PEL/06.

de Moor CL. 2019b. Sardine projections based on constant catch scenarios. DAFF: Branch Fisheries Document FISHERIES/2019/APR/SWG-PEL/07.

de Moor CL. 2020a. Final baseline assessment of the South African resource using data from 1984-2018. DEA: Branch Fisheries Document FISHERIES/2020/MAR/SWG-PEL/28.

de Moor CL. 2020b. Sardine projections based on constant catch scenarios. DEA: Branch Fisheries Document FISHERIES/2020/APR/SWG-PEL/33.

de Moor CL and Butterworth DS. 2009. Did High Directed Sardine TACs Cause the Rapid Decline in Sardine Abundance. Marine and Coastal Management Document: MCM/2009/SWG-PEL/10.

de Moor CL, Coetzee JC and Butterworth DS. 2019. Uncertainties and associated concerns relating to using short-term projections to advise on the 2020 sardine TAC and TABs. MARAM International Stock Assessment Workshop , 2-5 December 2019, Cape Town, Document MARAM/IWS/2019/Sardine/P3.

de Moor CL, Merkle D, Coetzee J and van der Lingen C. 2020. The data used in the 2020 sardine assessment. DEA: Branch Fisheries Document FISHEREIS/2020/MAR/SWG-PEL/29.

Table 1. The negative log likelihood and estimated parameter values when fitting a stock-recruitment relationship to the model estimated spawner biomass and November recruitment after conditioning.

	$-ln$	α_w^S	β_w^S	$\sigma_{r,w}^S$	$-lnL$	α_s^S	β_s^S	$\sigma_{r,s}^S$
Beverton Holt	38.56	21.81	21.28	0.81	91.12	7.31	1019.49	3.27
Hockey Stick	39.14	15.58	21.15	0.82	90.76	1.29	160.35	3.24
Ricker	39.21	0.48	0.008	0.82	91.08	0.008	0.001	3.27

Table 2a. Model predicted total biomass (without correction for survey bias), effective spawner biomass and May recruitment (without correction for survey bias) for the west component from this baseline assessment compared to that of de Moor (2019a) and de Moor (2020a).

	Total biomass			Effective spawner biomass			May recruitment		
	Current	de Moor (2020a)	de Moor (2019a)	Current	de Moor (2020a)	de Moor (2019a)	Current	de Moor (2020a)	de Moor (2019a)
1984	111.5	92.8	35.7	25.4	23.6	7.3			
1985	114.6	103.5	40.2	15.9	14.9	7.2	6.093	6.191	4.847
1986	217.7	205.3	132.7	35.5	39.1	18.1	5.434	6.009	5.463
1987	272.8	277.5	369.4	70.7	78.8	73.5	9.466	9.231	8.605
1988	346.5	345.5	352.8	59.7	67.1	40.6	0.814	0.842	0.741
1989	283.4	297.1	339.1	75.6	85.2	135.3	7.740	7.489	6.537
1990	214.5	222.6	258.8	59.2	70.3	117.1	3.075	3.074	2.994
1991	295.5	289.0	680.4	43.1	50.3	56.5	3.372	3.497	3.603
1992	499.2	459.1	380.5	47.9	51.4	54.1	13.554	14.336	8.423
1993	663.8	680.8	915.3	99.1	109.3	193.4	26.516	27.432	30.957
1994	500.7	483.1	506.4	118.2	131.4	202.1	4.221	4.364	4.492
1995	606.9	618.0	927.3	111.6	122.2	165.7	28.878	28.272	27.436
1996	770.4	739.4	618.1	92.6	105.4	48.2	5.565	5.871	4.600
1997	1029.4	1026.8	1592.0	116.9	131.0	151.0	38.229	40.447	39.663
1998	1034.1	1046.0	1311.6	113.1	130.1	128.0	32.352	31.299	26.329
1999	909.5	887.8	917.7	121.2	137.9	145.3	33.449	34.890	30.737
2000	1301.2	1154.3	1203.6	121.9	135.1	154.2	32.895	34.466	32.693
2001	1084.3	1007.5	1075.3	65.3	70.3	62.7	91.368	93.557	88.271
2002	1281.1	1152.3	1284.7	103.2	110.7	148.4	89.201	92.805	92.197
2003	1030.9	935.5	1334.6	158.9	164.7	204.1	82.249	81.988	85.584
2004	316.9	295.5	312.6	211.3	216.8	211.5	10.584	11.309	11.942
2005	176.6	158.7	144.7	79.8	80.6	73.7	7.275	7.330	6.849
2006	176.3	170.0	216.6	46.7	49.5	47.7	9.555	10.008	11.702
2007	99.8	96.9	87.0	23.3	25.2	16.8	5.099	5.258	4.748
2008	182.2	153.6	193.4	22.8	25.2	24.1	10.350	12.322	13.177
2009	438.6	382.6	322.6	40.7	43.3	88.2	9.546	8.047	10.452
2010	242.9	251.7	399.3	66.3	62.6	72.5	18.436	17.125	20.602
2011	328.8	356.8	506.3	69.9	79.6	150.6	8.999	12.124	9.756
2012	425.7	455.2	861.8	96.0	127.1	143.3	12.446	13.280	7.280
2013	122.3	125.9	191.4	53.5	62.7	90.9	7.076	6.723	12.076
2014	221.0	227.1	390.7	39.8	44.8	98.7	2.991	3.160	3.849
2015	92.4	102.1	96.2	40.4	47.9	63.9	6.147	6.341	8.057
2016	176.1	215.7	219.5	34.8	38.8	38.2	2.880	3.056	3.162
2017	99.3	97.0	110.9	45.4	33.5	33.1	4.079	6.612	7.373
2018	40.1	51.1	56.7	18.3	25.1	21.0	1.837	13.348	16.395
2019	89.7			21.5			7.637		

Table 2b. Model predicted total biomass (without correction for survey bias), effective spawner biomass and May recruitment (without correction for survey bias) for the south component from this baseline assessment compared to that of de Moor (2019a) and de Moor (2020a).

	Total biomass			Effective spawner biomass			May recruitment		
	Current	de Moor (2020a)	de Moor (2019a)	Current	de Moor (2020a)	de Moor (2019a)	Current	de Moor (2020a)	de Moor (2019a)
1984	0.5	0.5	0.5	0.3	0.3	0.3			
1985	45.7	47.7	98.2	10.1	10.6	21.2	<0.0001	<0.0001	<0.0001
1986	38.7	38.2	41.5	24.7	23.7	20.2	<0.0001	<0.0001	<0.0001
1987	18.4	18.6	20.2	12.9	13.1	13.1	0.028	0.034	<0.0001
1988	12.3	12.2	9.8	4.7	4.8	3.0	0.219	0.204	0.036
1989	64.8	61.4	72.3	21.3	20.5	25.4	<0.0001	<0.0001	0.188
1990	61.6	71.9	63.9	21.7	23.3	22.0	0.919	1.276	0.817
1991	90.1	96.8	111.2	25.7	28.5	27.6	2.101	2.175	<0.0001
1992	157.4	163.1	158.9	44.3	47.7	57.0	1.529	0.186	0.885
1993	174.7	176.1	147.7	53.7	54.6	46.6	3.286	3.028	0.011
1994	240.4	240.5	269.0	97.5	94.9	93.0	1.021	1.006	1.204
1995	131.6	139.2	187.6	61.0	61.9	69.6	0.399	0.402	0.624
1996	299.0	299.0	269.2	55.4	58.0	43.9	8.382	8.087	1.117
1997	292.0	293.4	458.4	81.6	78.7	85.5	<0.0001	<0.0001	<0.0001
1998	611.9	629.5	538.1	141.3	143.3	87.3	0.476	0.482	0.728
1999	987.4	1039.3	1216.4	248.9	258.6	244.9	2.320	2.410	4.400
2000	1110.6	1160.1	1247.7	289.3	300.6	275.8	10.139	9.880	11.687
2001	2375.4	2504.6	2716.4	424.9	440.8	409.5	0.001	0.001	0.001
2002	3127.2	3329.5	3847.5	728.1	749.6	693.4	2.403	2.410	3.666
2003	2641.1	2874.6	3073.5	770.2	813.0	695.1	0.790	0.797	1.240
2004	1814.7	1875.6	1882.9	1186.4	1216.2	1026.6	1.043	1.048	1.705
2005	833.9	864.4	767.3	562.0	587.8	479.2	1.019	1.029	1.770
2006	405.5	424.4	376.4	230.3	243.9	185.1	4.899	4.767	8.486
2007	330.0	342.5	296.2	164.3	166.7	109.3	2.528	2.510	4.703
2008	306.7	323.9	238.9	133.3	137.8	78.0	3.255	1.848	0.633
2009	349.6	326.0	462.5	156.9	149.9	175.0	3.255	3.350	8.616
2010	577.9	550.9	419.0	267.4	250.3	158.2	0.540	0.569	0.946
2011	288.4	293.5	341.2	204.7	198.2	155.6	<0.0001	<0.0001	0.207
2012	161.4	169.8	213.1	84.5	92.4	88.9	2.979	2.804	4.653
2013	386.8	396.2	346.7	188.4	193.6	169.0	0.348	0.368	0.602
2014	278.1	283.3	342.6	157.6	157.6	158.3	3.234	3.047	1.870
2015	287.0	284.0	342.5	160.3	159.1	179.7	1.312	1.264	3.708
2016	149.4	167.5	88.4	91.4	90.9	34.5	0.974	0.796	1.506
2017	305.7	476.1	315.8	154.7	216.2	121.1	4.349	5.444	7.590
2018	349.5	560.0	382.2	135.1	203.3	127.8	10.110	8.715	14.880
2019	385.0			169.5			13.464		

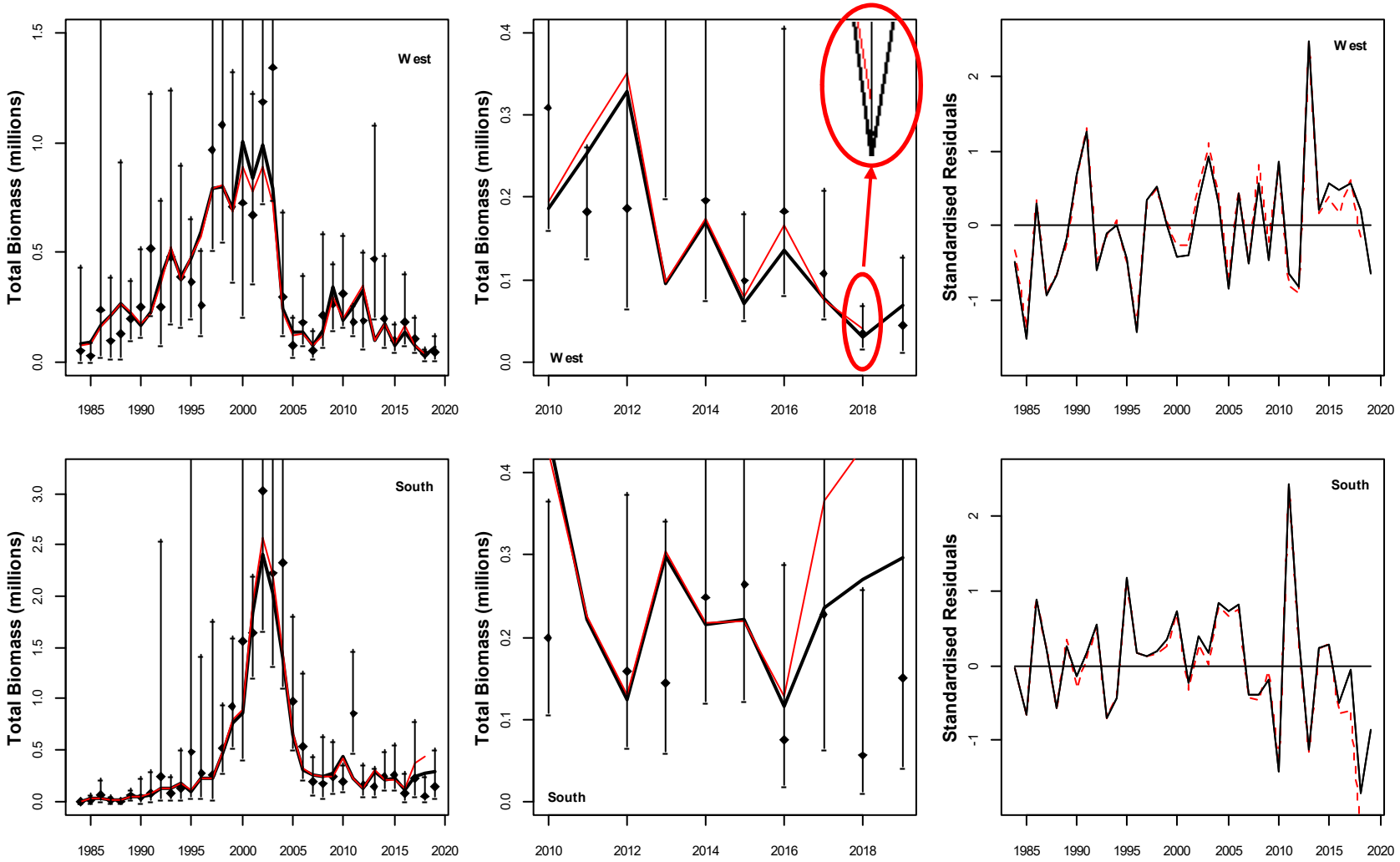

Figure 1. Acoustic survey estimated and model predicted November sardine total biomass from 1984 to 2019. The observed indices are shown with 95% confidence intervals. The centre plot shows only the most recent 10 years of the left hand plot. The standardised residuals (i.e. the residual divided by the corresponding standard deviation, including additional variance where appropriate) from the fits are given in the right hand plots. The red lines indicate the November biomass predicted by de Moor (2020a) and associated residuals.

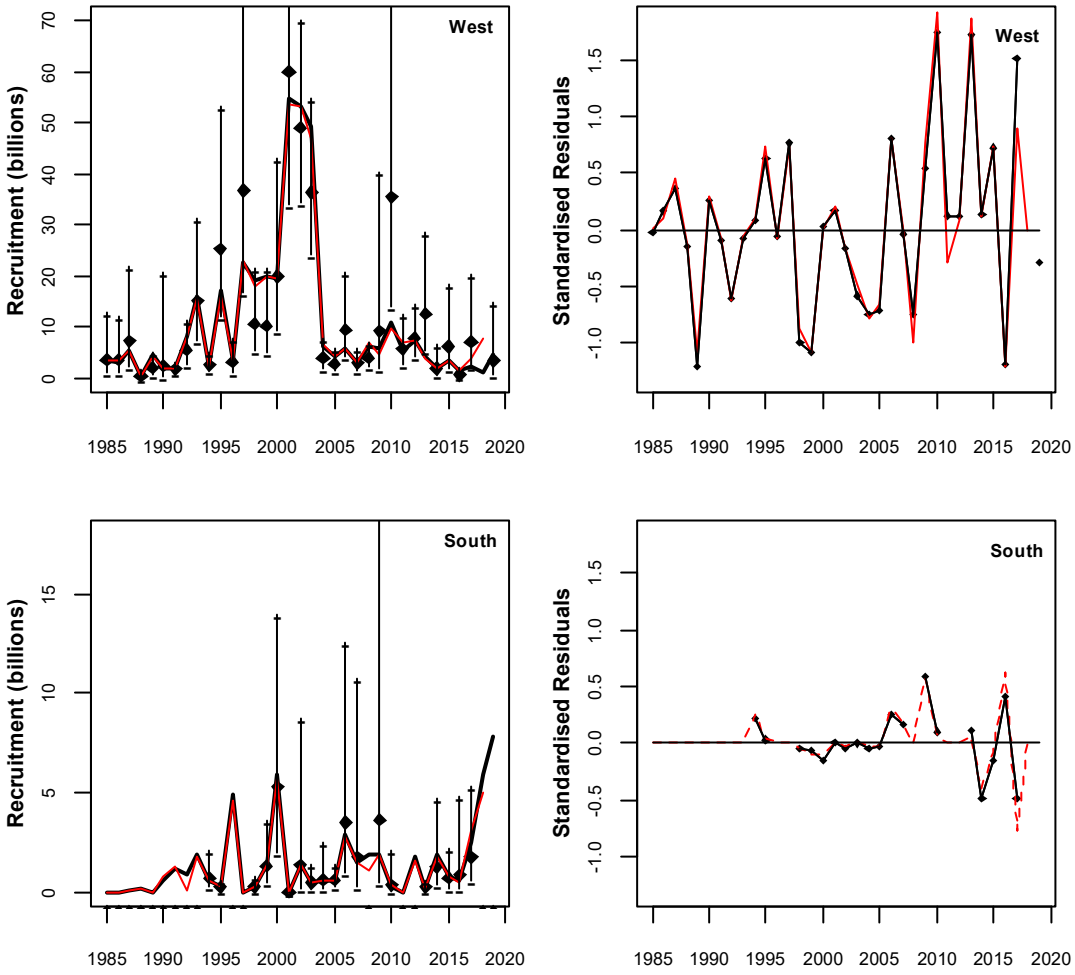

Figure 2. Acoustic survey estimated and model predicted sardine recruitment numbers from May/June 1985 to 2019. There was no survey observation in 2018; the model predicted value corresponds to the recruitment predicted at 8th June 2018 which is the average start date of the survey from 2016, 2017 and 2019 surveys. The survey indices are shown with 95% confidence intervals. The standardised residuals from the fit are given in the right hand plots. The red lines indicate the May recruitment predicted by de Moor (2020a) and associated residuals.

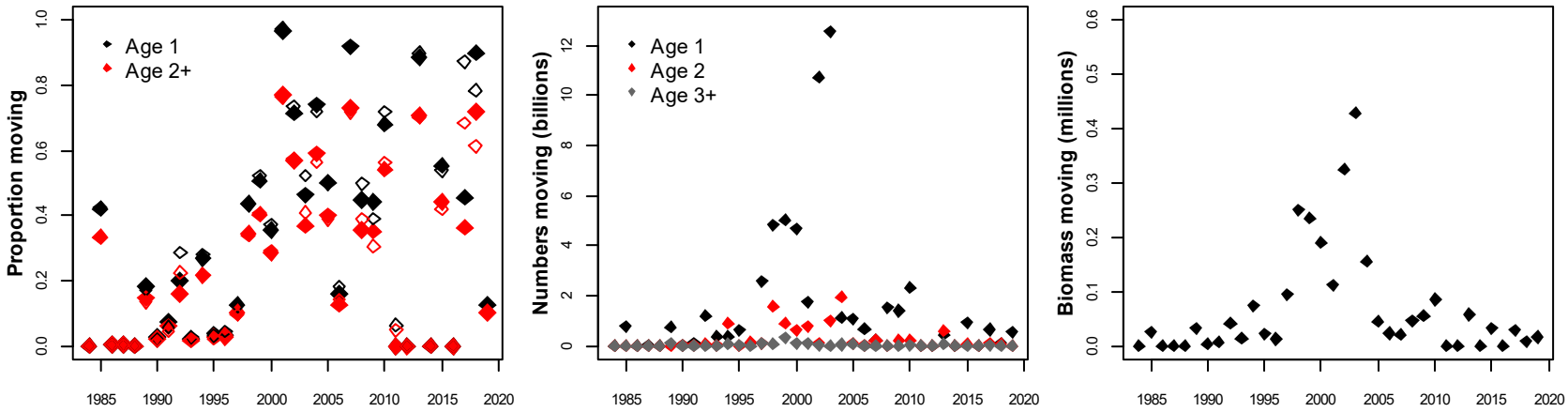

Figure 3. Model estimated proportion of 1-year-olds and 2+-year-olds which move from the west component to the south component in November. The middle plot shows the numbers of 1-, 2- and 3-year olds moving while the right hand plot shows rough[1] estimates of the annual biomass moving from the west to south component. The open diamonds in the left plot indicate the proportions estimated by de Moor (2020a).

[1] Calculated using the average of west and south component weights-at-age.

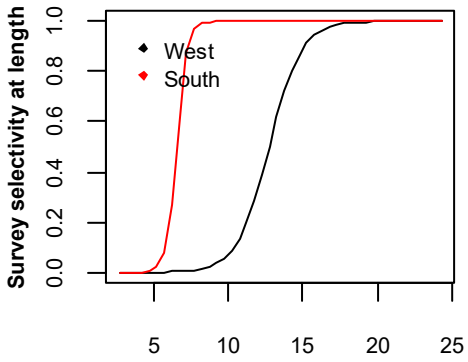

Figure 4. The model estimated November survey selectivity at length.

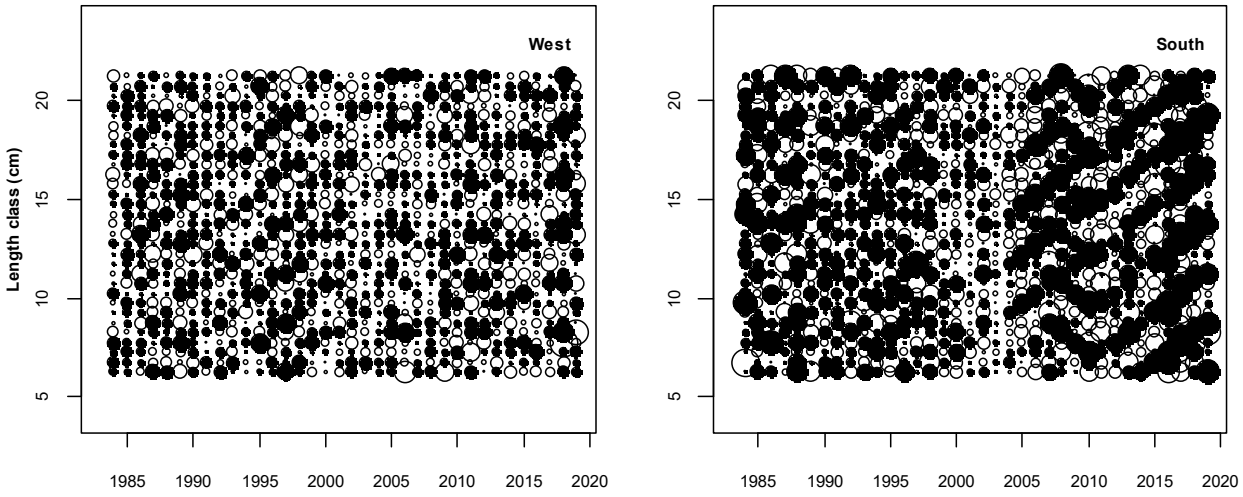

Figure 5. Residuals from the fit of the model predicted proportions-at-length in the November survey to the hydroacoustic survey estimated proportions.

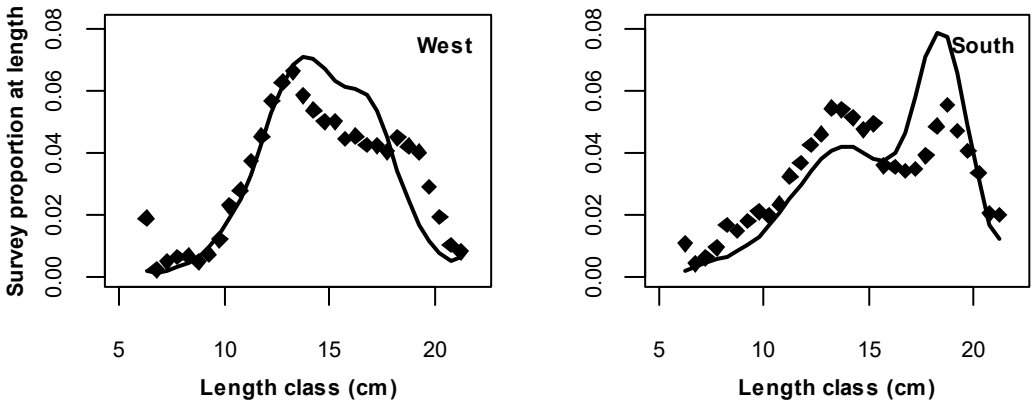

Figure 6. Average (over all years) model predicted and observed proportion-at-length in the November survey.

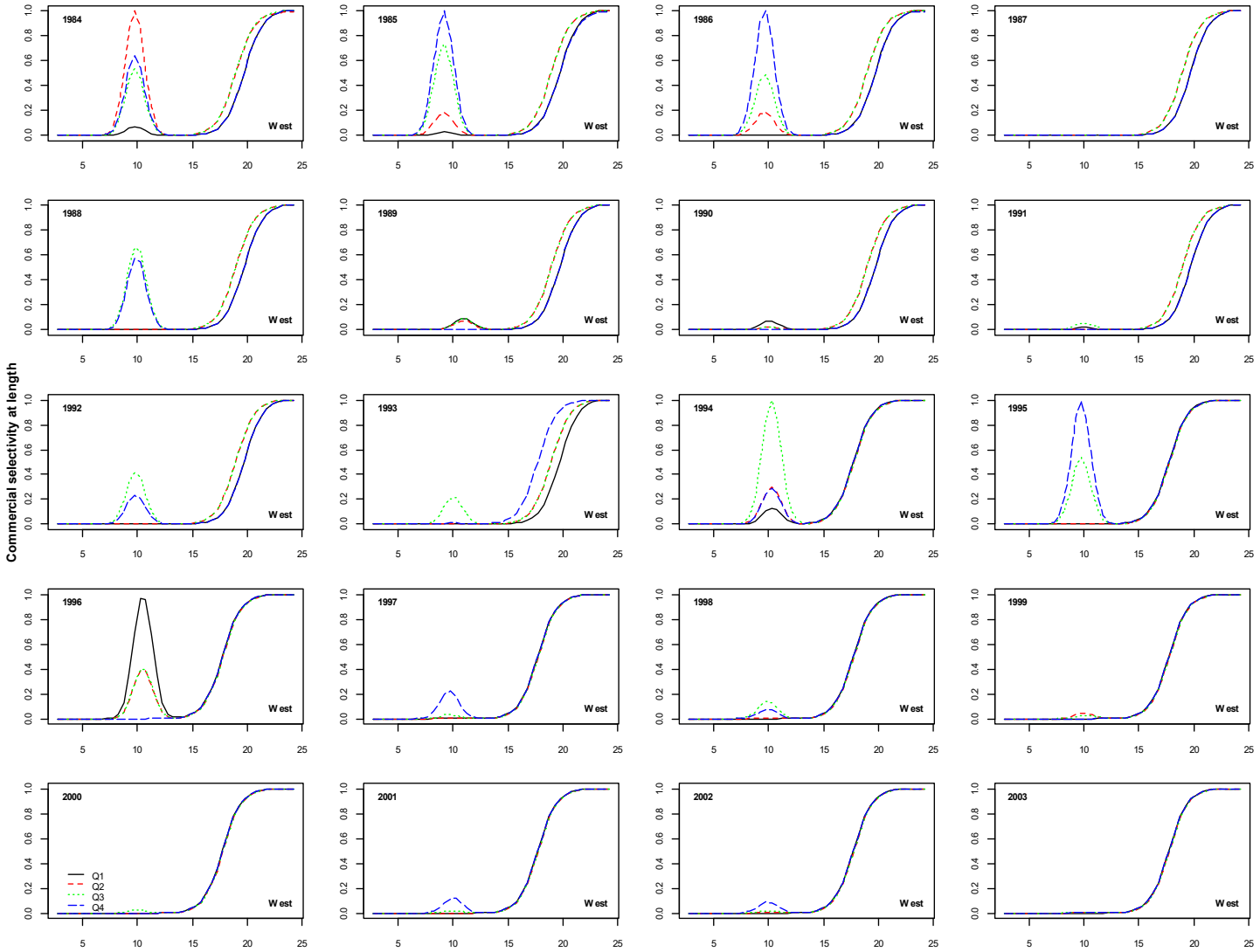

Figure 7. The model estimated commercial selectivity at length.

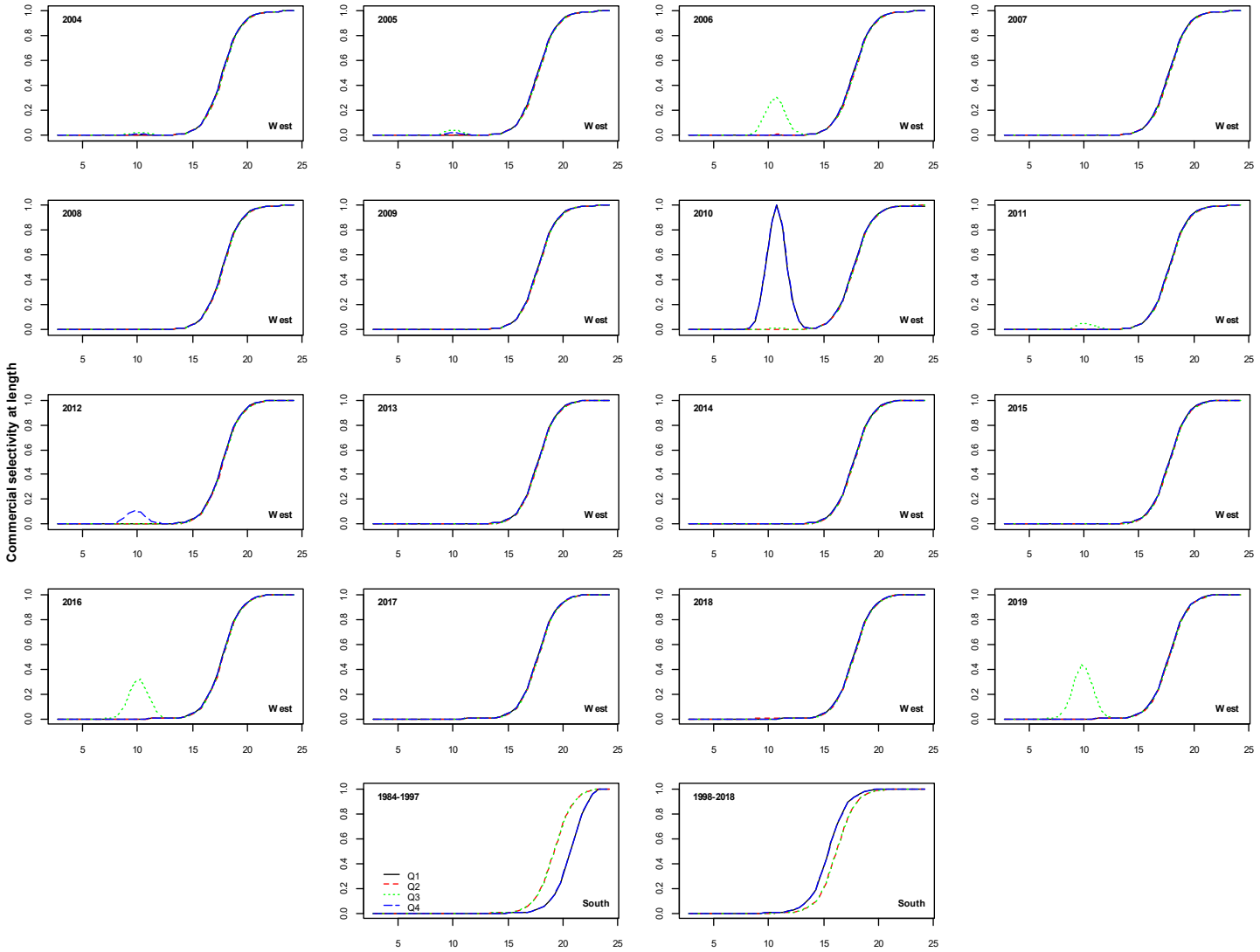

Figure 7 (continued).

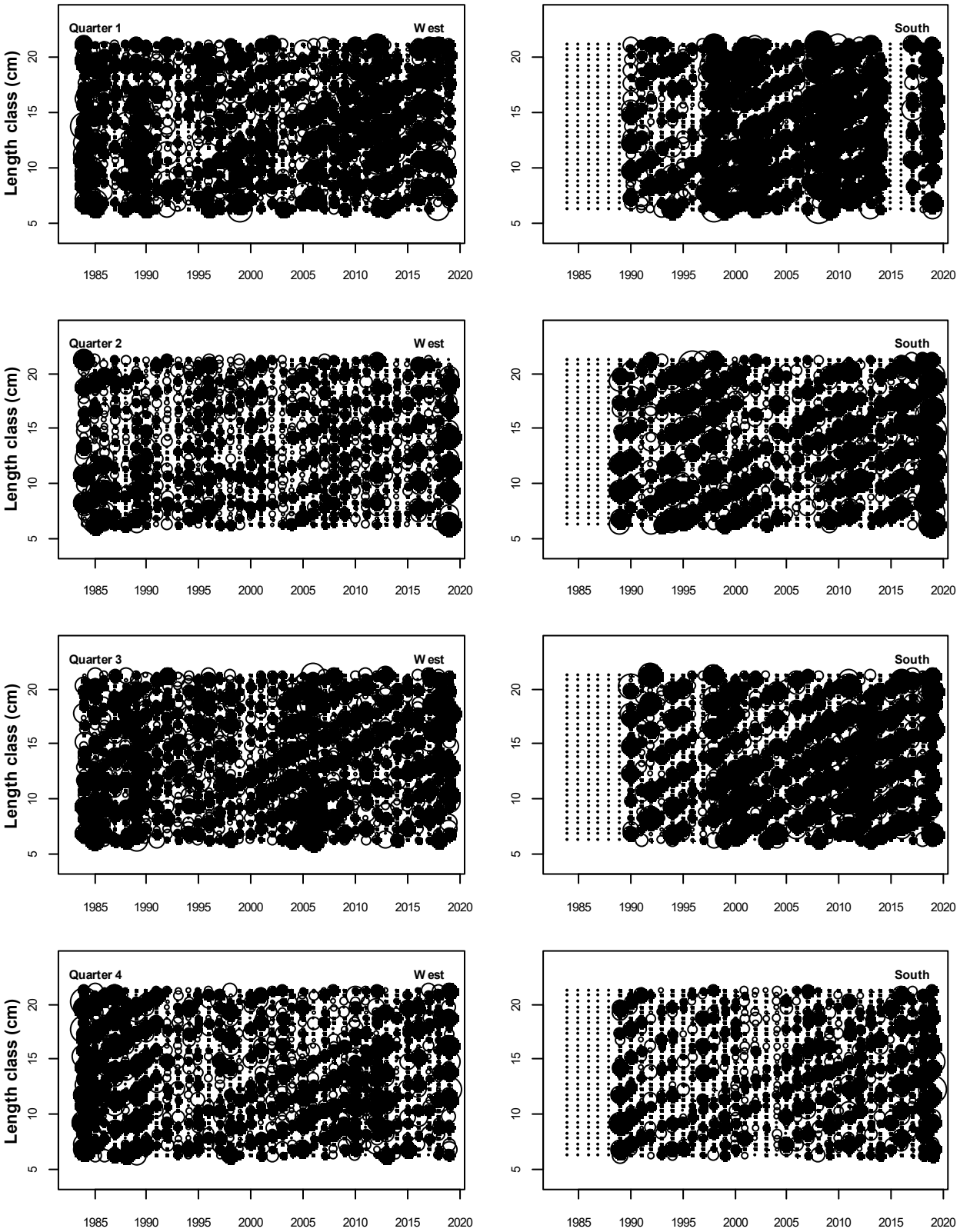

Figure 8. Residuals from the fit of the model predicted proportions-at-length in the quarterly commercial catch to the observed proportions.

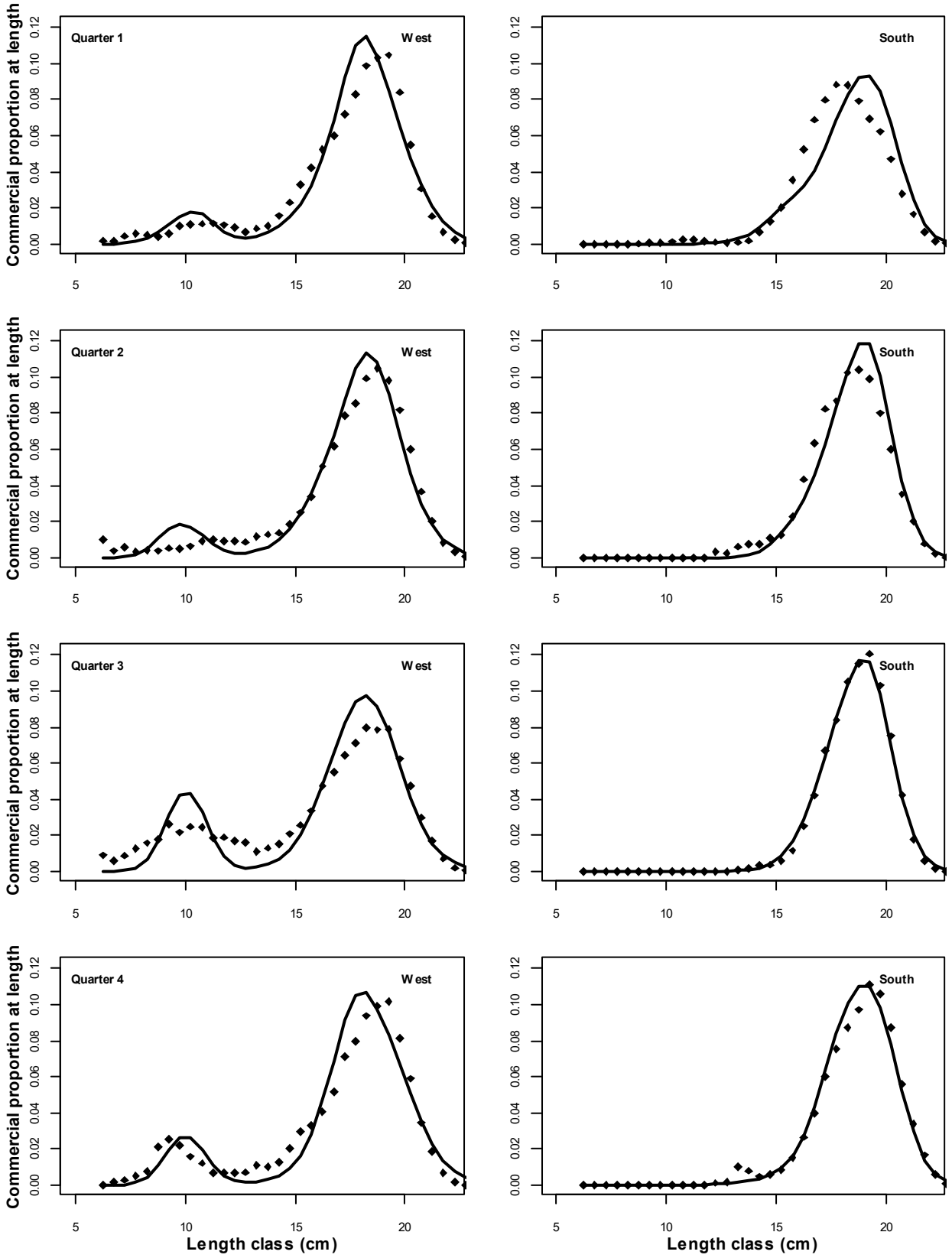

Figure 9. Average (over all quarters and years) model predicted and observed proportion-at-length in the commercial catch (top row), and average (over all years) quarterly model predicted and observed proportions-at-length in the commercial catch (subsequent rows). See Appendix B for plots for each year and quarter.

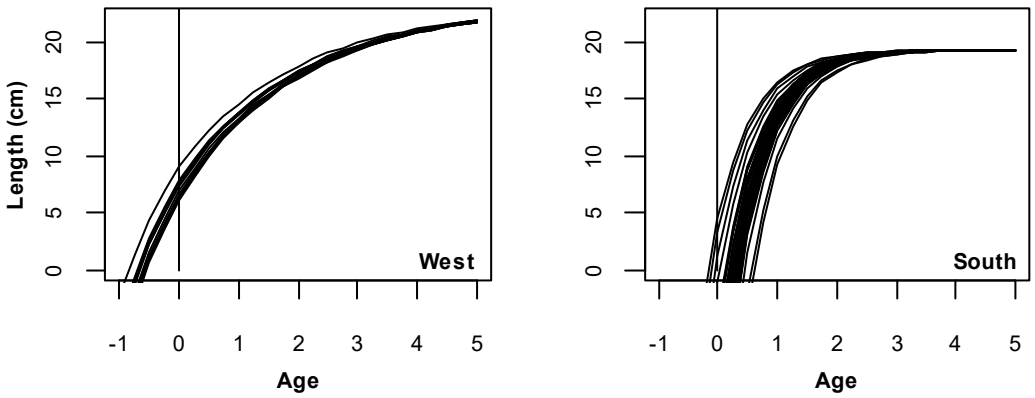

Figure 10. The von Bertalanffy growth curves (by cohort) estimated by allowing for auto-correlated residuals for the variation about the age at which length is zero.

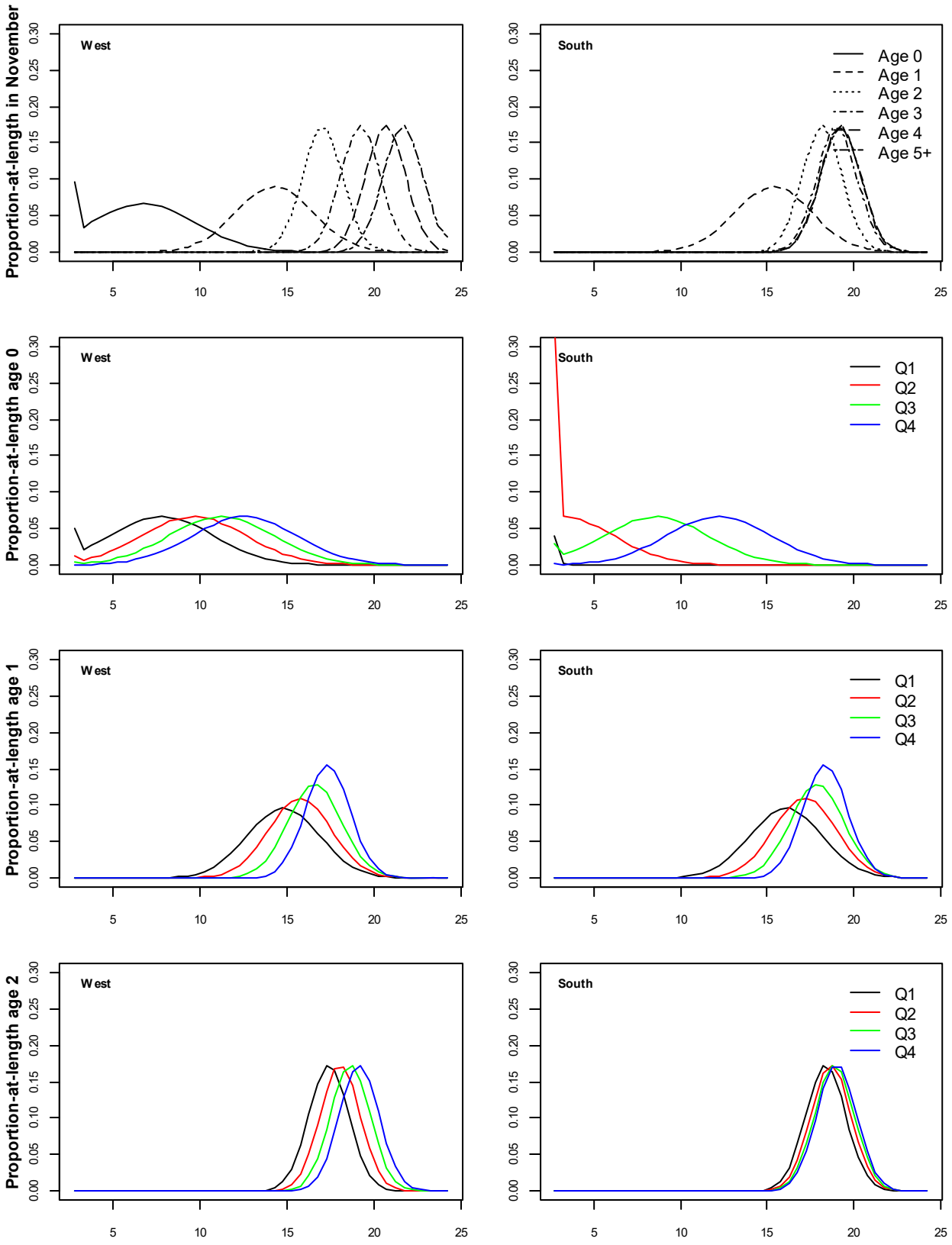

Figure 11. The model estimated distributions of proportions-at-length for each age **in 2010**, given at the time of the biomass survey (1 November, top row), and middle of each quarter of the year (corresponding to the times commercial catch is modelled to be taken) for age 0, 1 and 2 (subsequent rows).

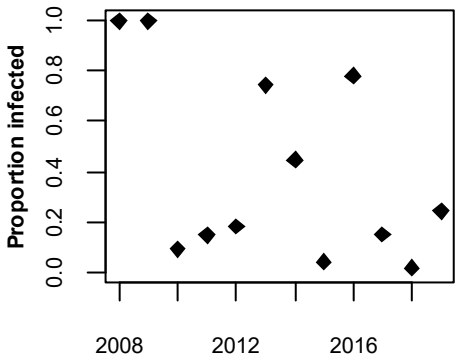

Figure 12. The model estimated proportion of west component sardine infected with the parasite between 2008 and 2019. (Annual infection rate is arbitrarily assumed to be 0 prior to 2008.)

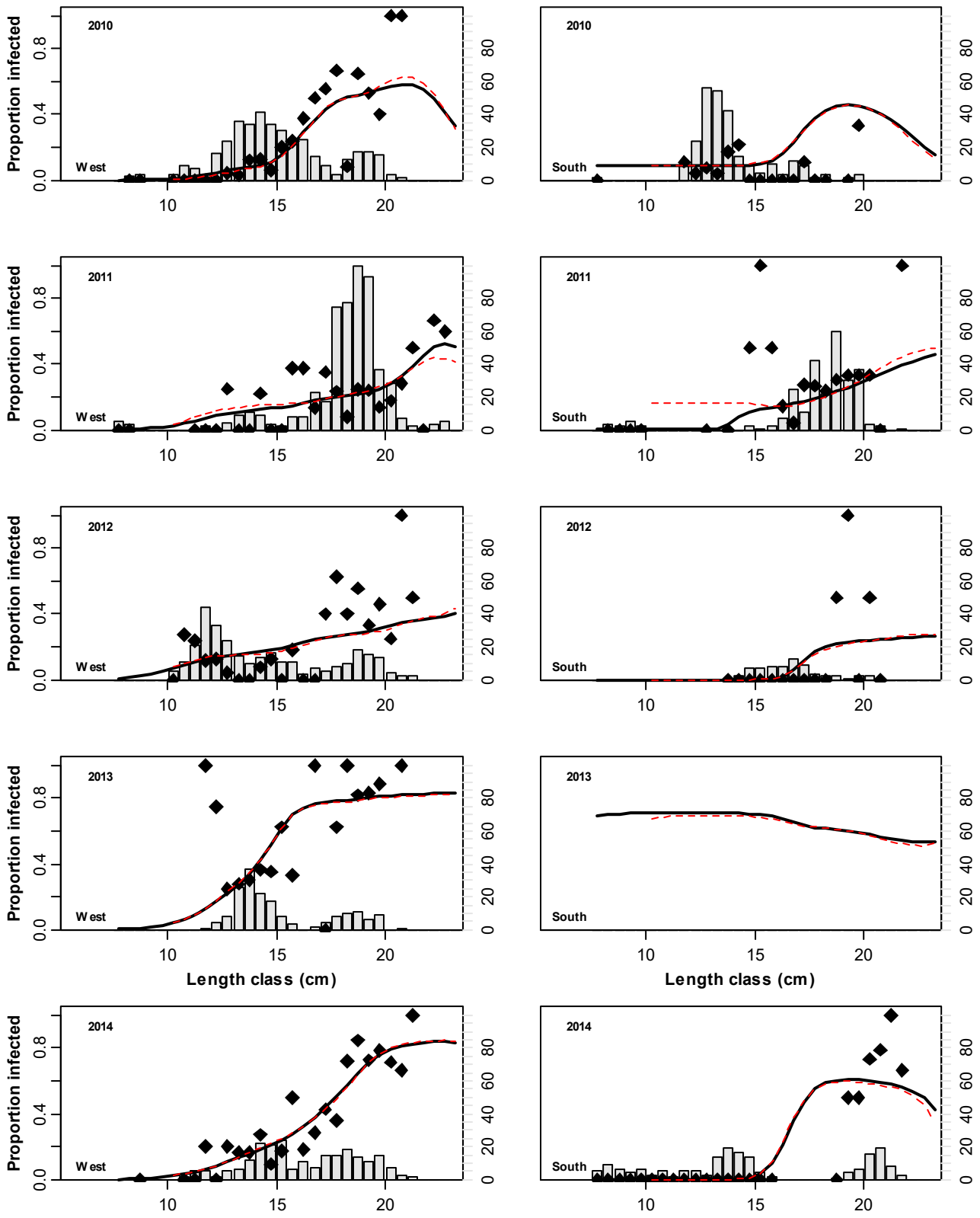

Figure 13. The model estimated proportions-at-length of west and south stock sardine infected with the parasite (i.e. parasite prevalence-by-length) between 2010 and 2019 together with the observed proportions-at-length. The red dashed line indicates the proportions predicted by de Moor (2020a). The sample size for each length class is given by the grey bars, plotted against the right vertical axis.

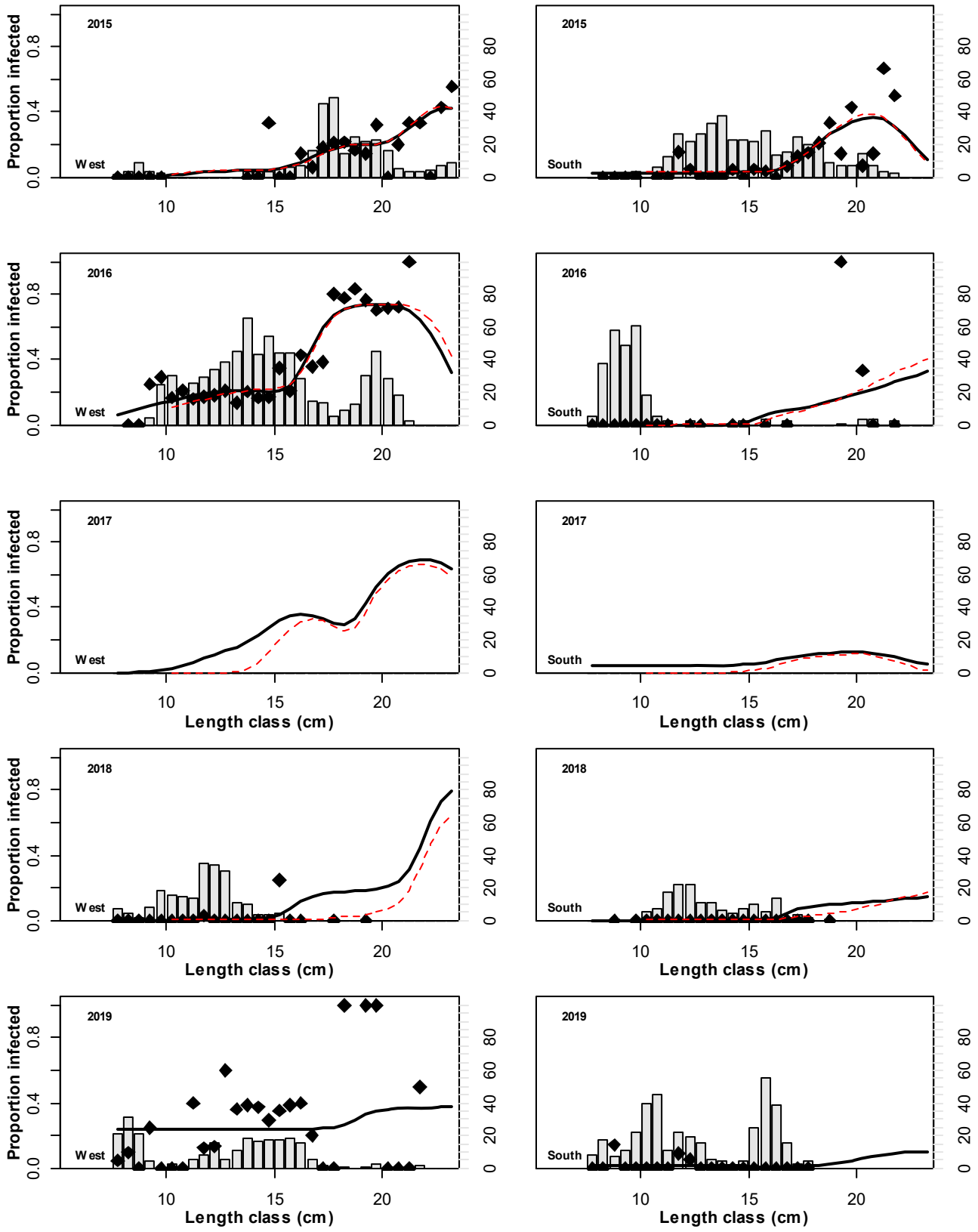

Figure 13 (continued).

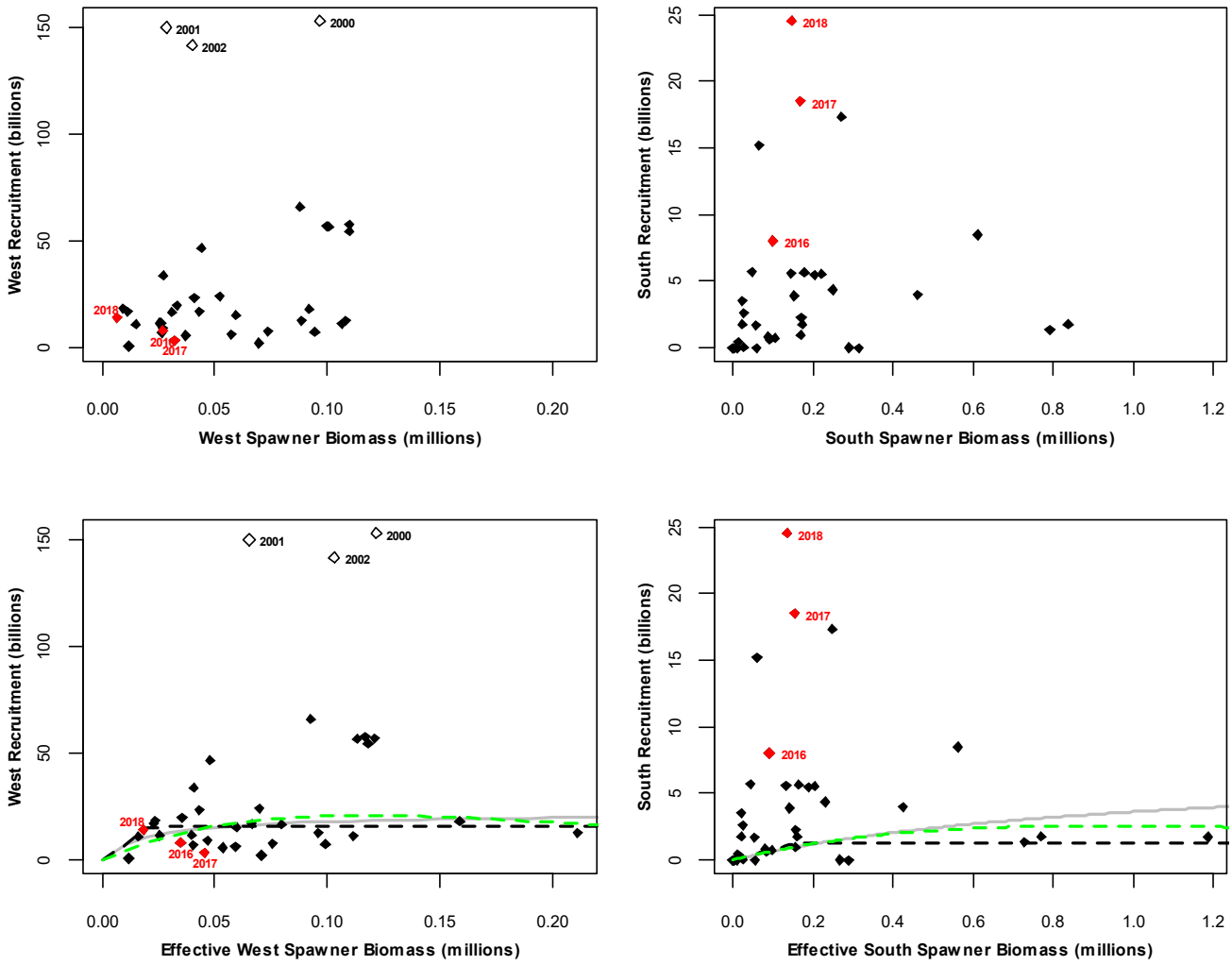

Figure 14. Model predicted sardine recruitment (in November) plotted against spawner biomass (top panels) and effective spawner biomass (lower panels) from November 1984 to November 2017. The open diamonds indicate the years of peak west component recruitment. The Hockey Stick (black), Beverton Holt (grey) and Ricker (green) stock recruitment relationships estimated after conditioning are also shown.

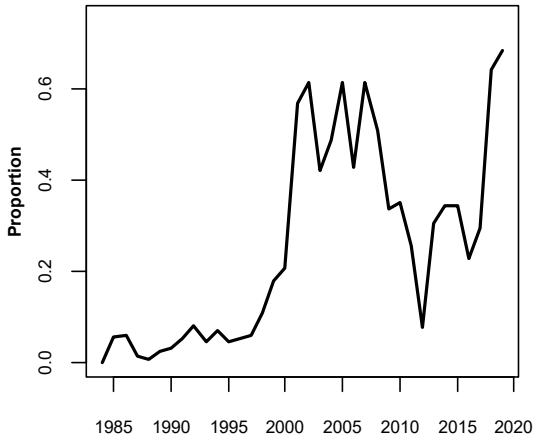

Figure 15. The proportion of west component effective spawner biomass (defined as west component spawner biomass combined with 8% of south component spawner biomass) that consists of south component spawner biomass (i.e. $SSB^{S}_{j=S,y}/SSB^{eff,S}_{j=W,y}$).

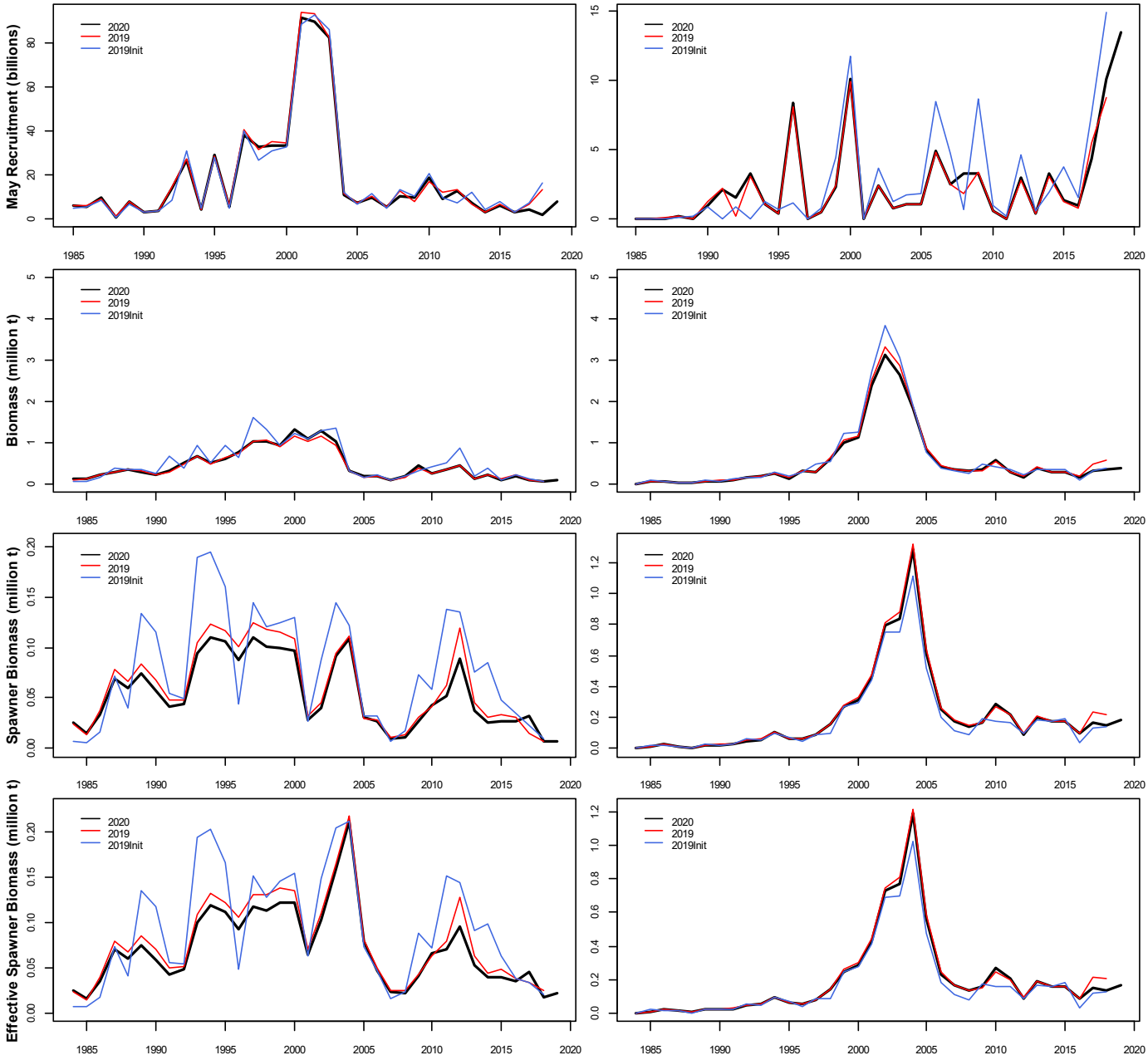

Figure 16. Model predicted May recruitment (without correction for survey bias), total biomass (without correction for survey bias), spawner biomass and effective spawner biomass and for the west and south components from this baseline assessment ("2020") compared to that of de Moor (2020a) ("2019") and de Moor (2019a) ("2019Init").

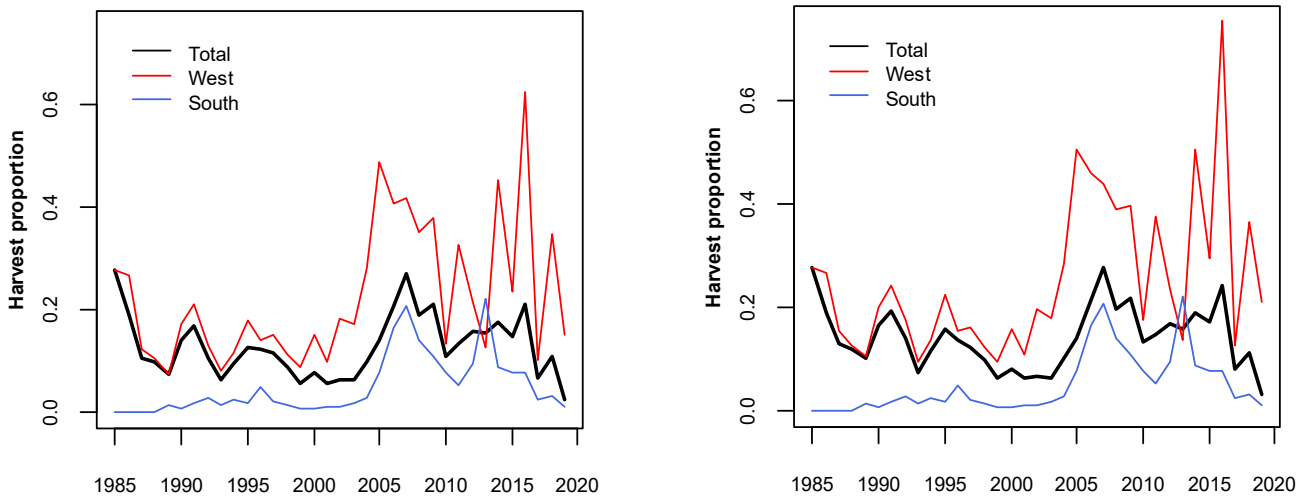

Figure 17. The exploitation rate (simply calculated as the observed annual (Nov-Oct) catch tonnage as a proportion of the model predicted total biomass). The left plot excludes small sardine bycatch with anchovy while the right plot includes these landings.

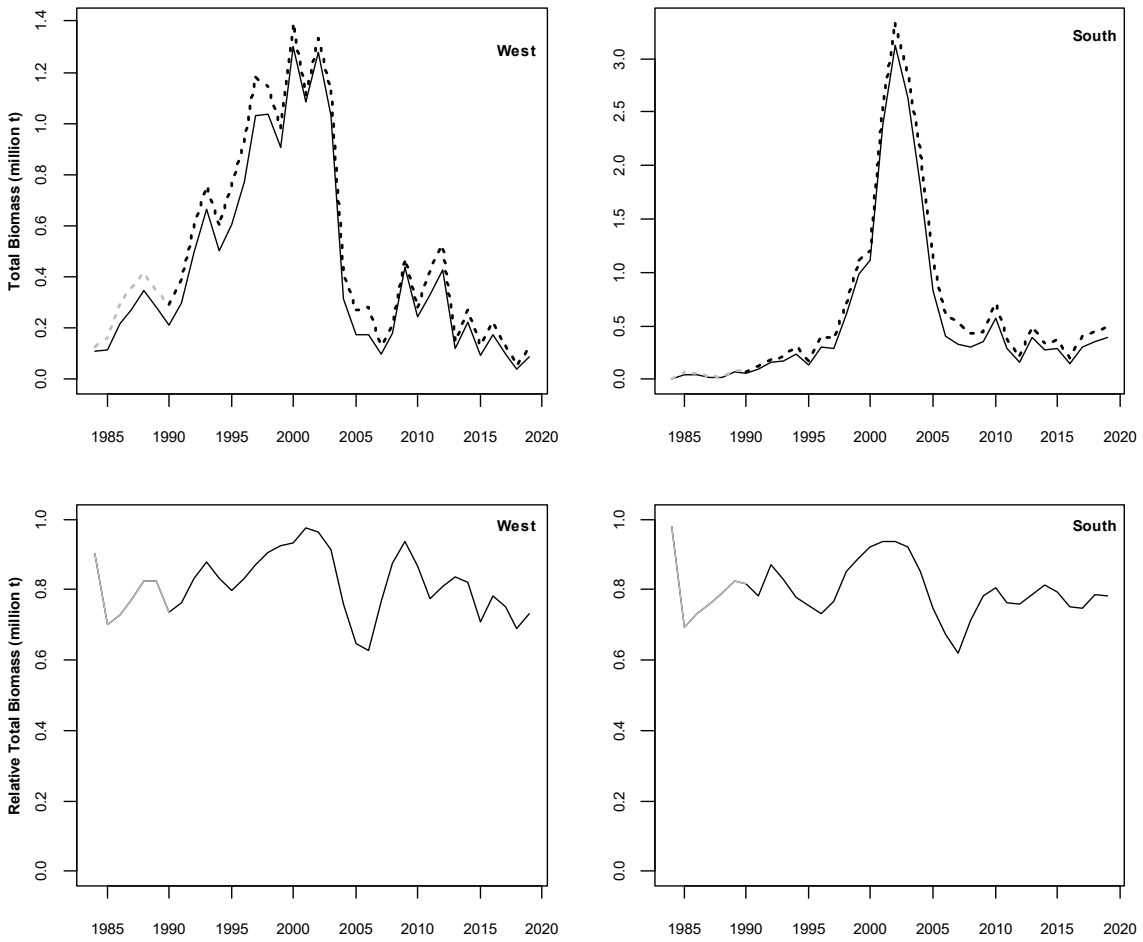

Figure 18a. The historical total sardine biomass under the baseline model (solid) and that calculated assuming no historical catch (Dynamic B_0) (dashed). The historical biomass relative to the Dynamic B_0 time series is also shown. The initial years are less reliable due to transient effects and are plotted in grey.

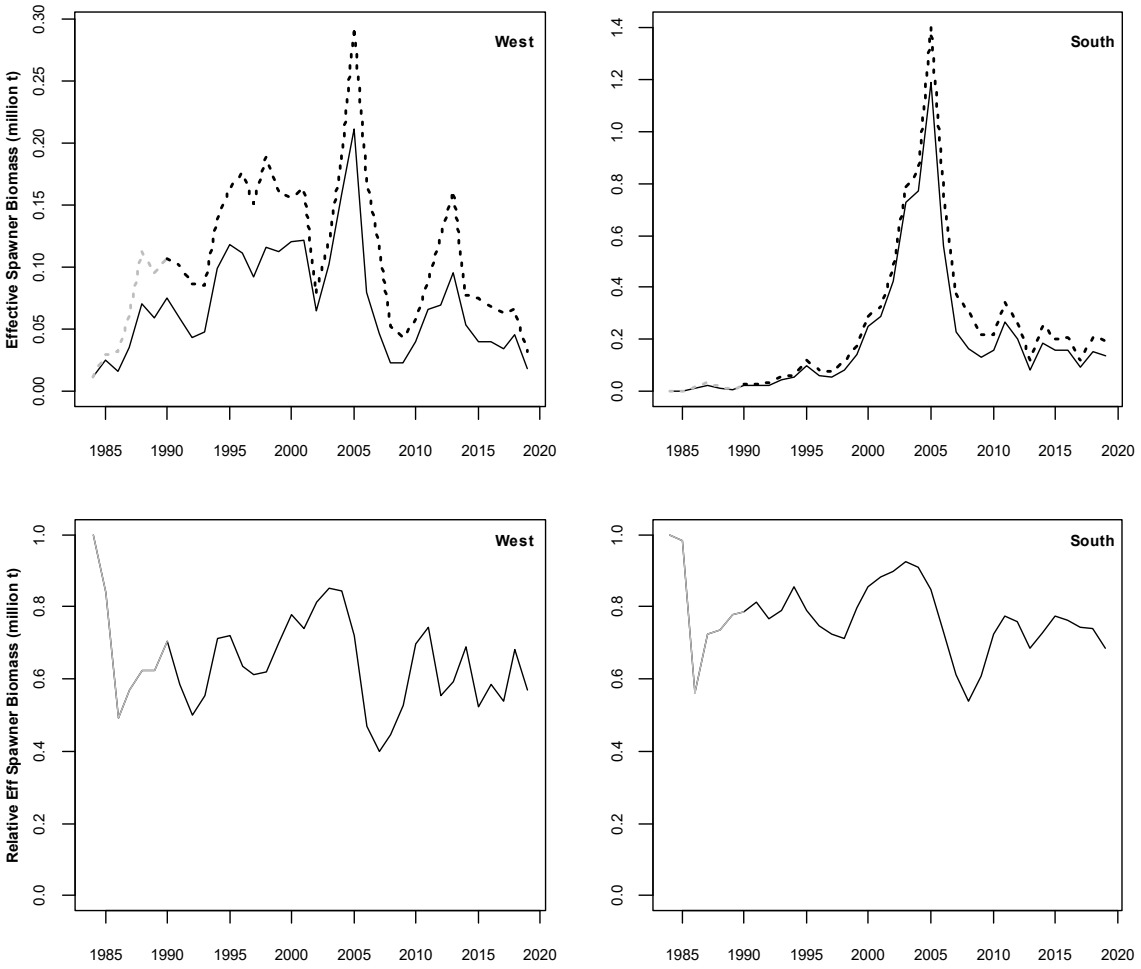

Figure 18b. The historical sardine effective spawner biomass under the baseline model (solid) and that calculated assuming no historical catch (Dynamic B_0) (dashed). The historical effective spawner biomass relative to the Dynamic B_0 time series is also shown. The initial years are less reliable due to transient effects and are plotted in grey.

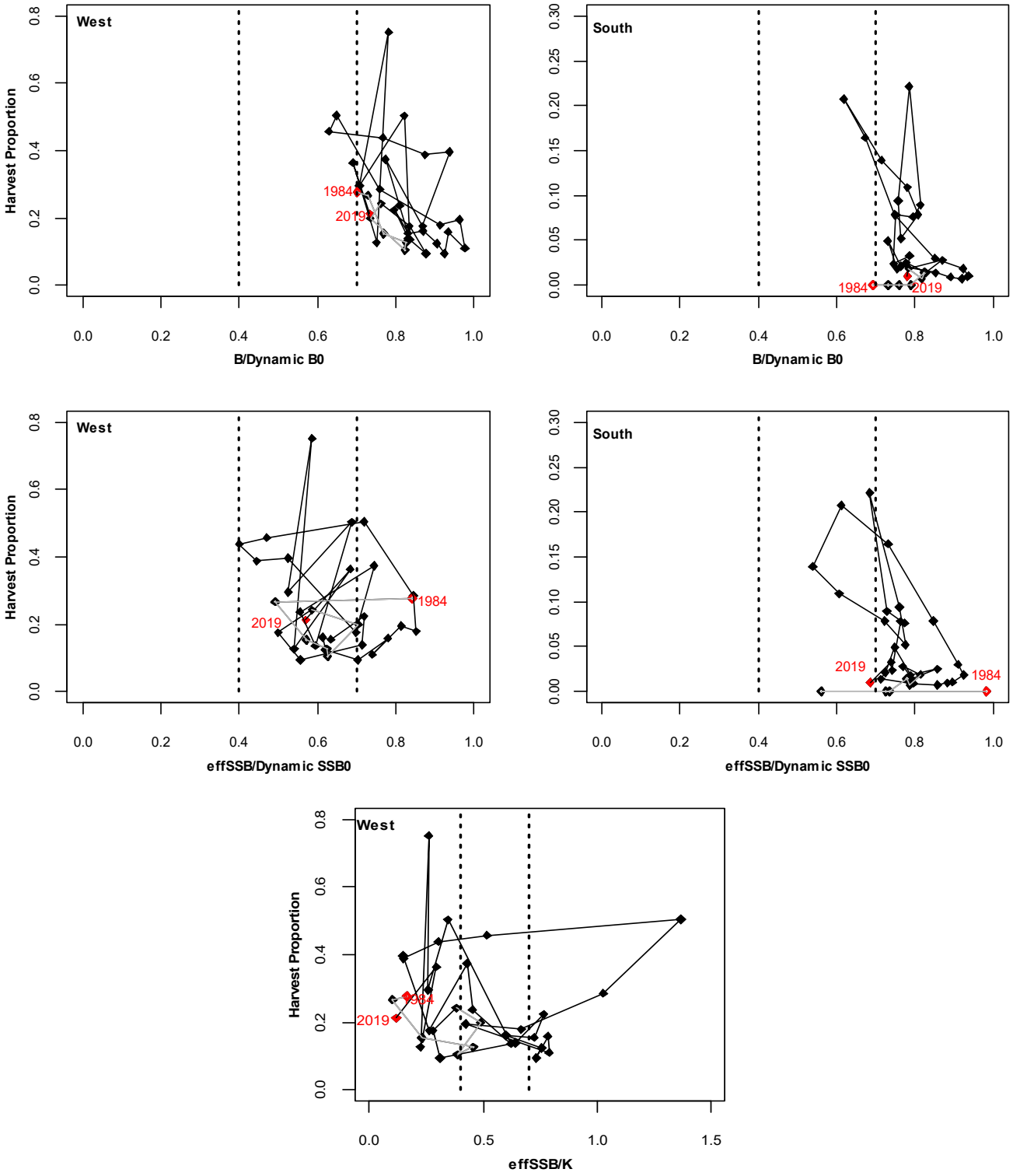

Figure 17. The historical harvest proportion plotted against the ratio of biomass to Dynamic B_0 (upper panels) and the ratio of effective spawner biomass to that calculated from the Dynamic B_0 model (middle panels). The initial years are less reliable due to transient effects and are shown by grey lines / open diamonds. The lower panel shows the equivalent figure using carrying capacity for the west component[2]. The dashed lines correspond to 40% and 70% of Dynamic B_0/carrying capacity. Note the vertical axes differ between the west and south components.

[2] The equivalent figure for the south component is not shown as migration from the west component into the south component has been a key influence to the south component biomass compared to south component recruitment and carrying capacity.

Appendix A: Detailed comparison between model predicted and observed commercial length frequencies

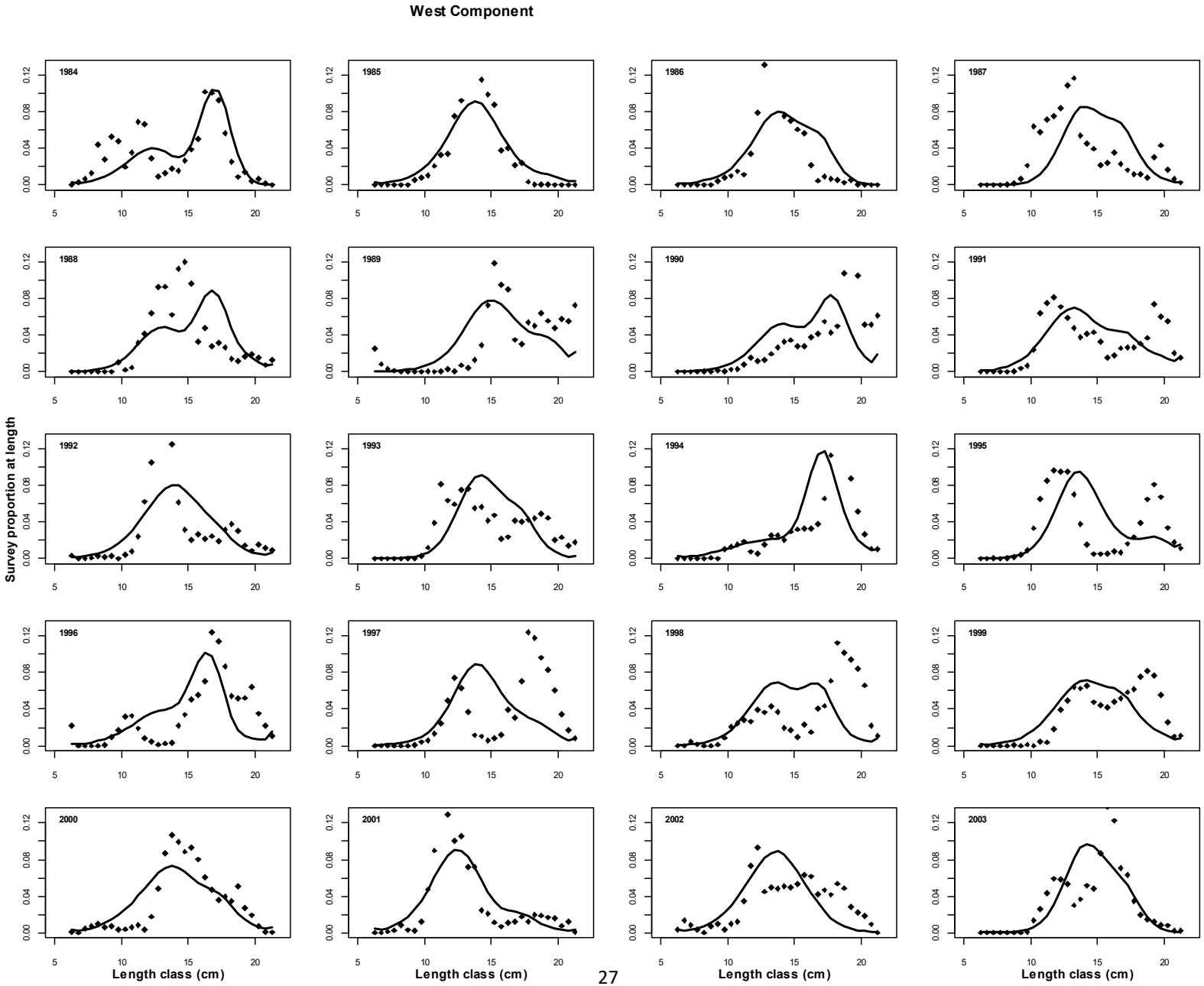
West Component
1984
1985
1986
1987
1988
1989
1990
1991
1992
1993
1994
1995
1996
1997
1998
1999
2000
2001
2002
2003
Survey proportion at length
Length class (cm)
Length class (cm)
Length class (cm)
Length class (cm)

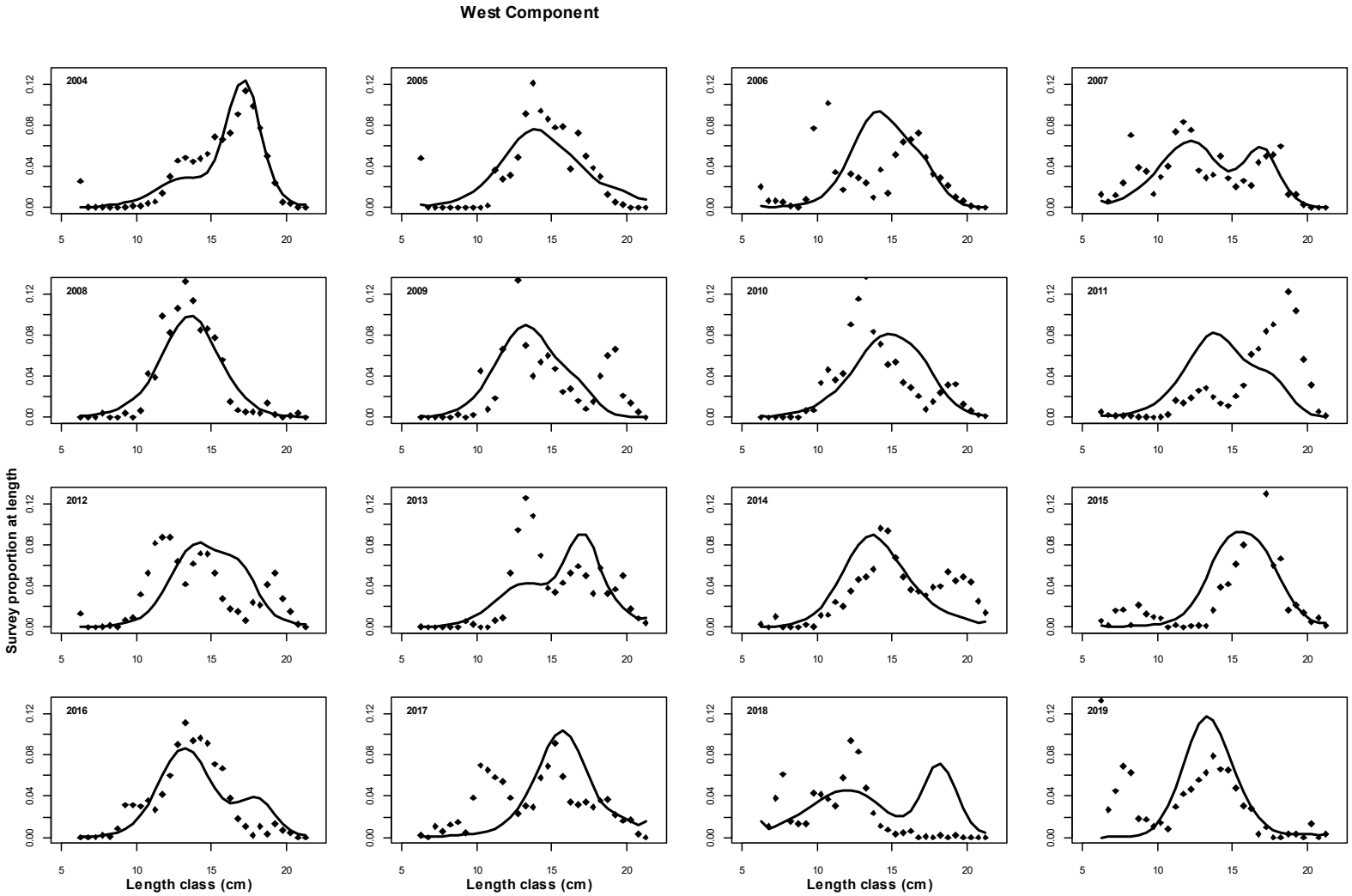
West Component
2004
2005
2006
2007
2008
2009
2010
2011
2012
2013
2014
2015
2016
2017
2018
2019
Survey proportion at length
Length class (cm)
Length class (cm)
Length class (cm)

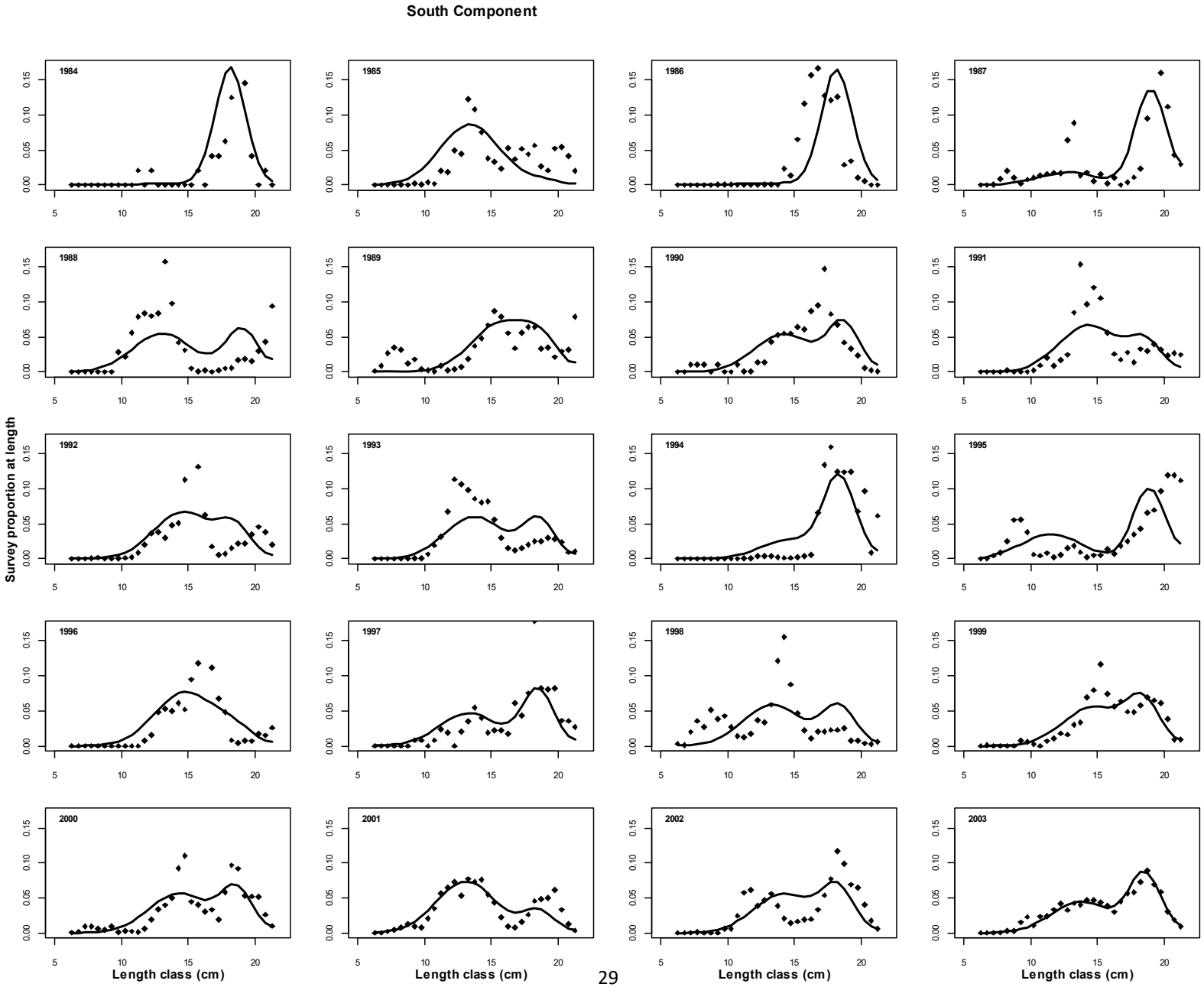
South Component
1984
1985
1986
1987
1988
1989
1990
1991
1992
1993
1994
1995
1996
1997
1998
1999
2000
2001
2002
2003
Survey proportion at length
Length class (cm)
Length class (cm)
Length class (cm)
Length class (cm)

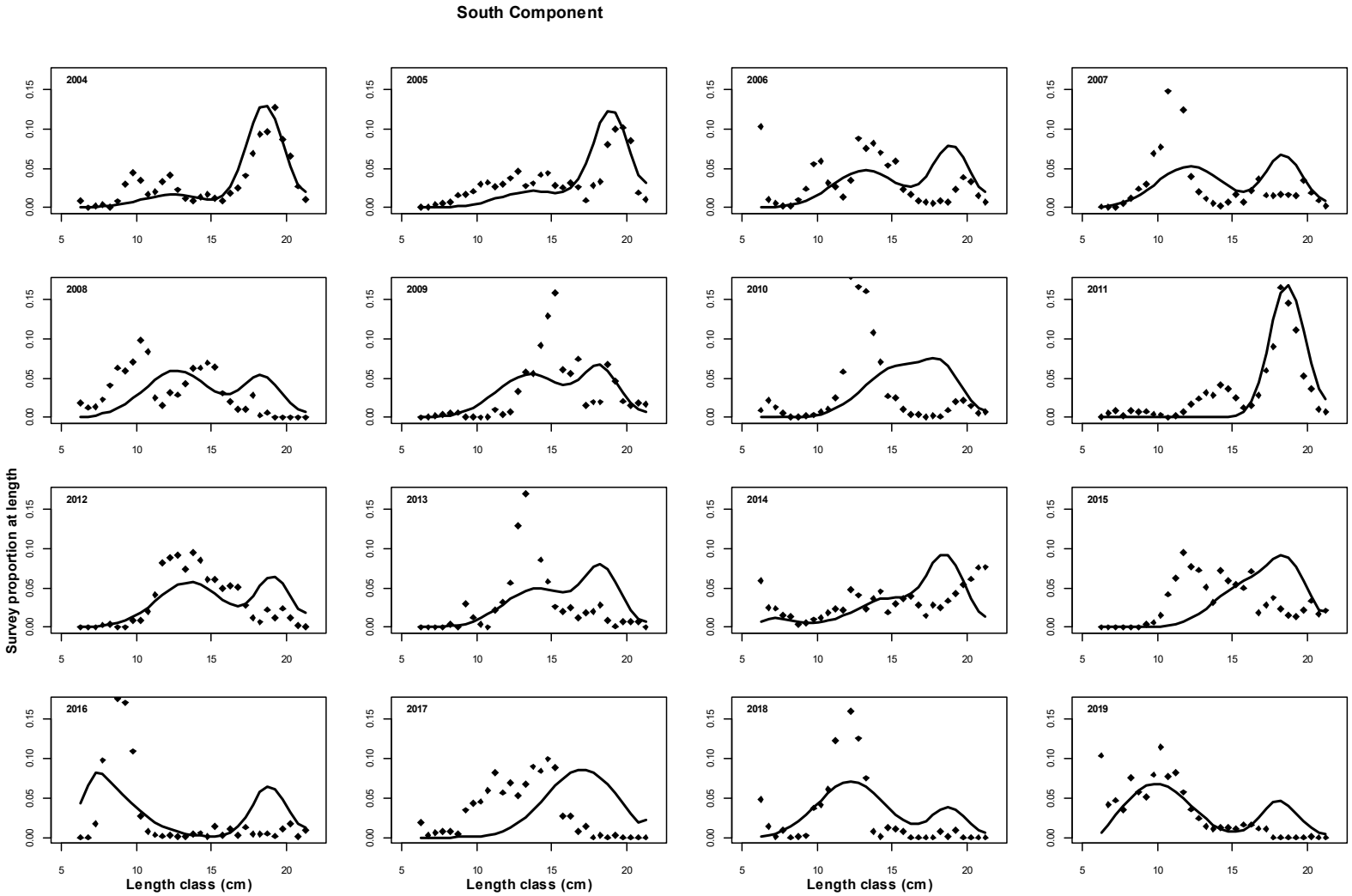
South Component
2004
2005
2006
2007
2008
2009
2010
2011
2012
2013
2014
2015
2016
2017
2018
2019
Survey proportion at length
Length class (cm)
Length class (cm)
Length class (cm)